Robust Sequential Phase Estimation using Multi-temporal SAR Image Series

Dana El Hajjar, Guillaume Ginolhac, Yajing Yan, Mohammed Nabil El Korso

Robust sequential phase estimation using Multi-temporal SAR image series

Dana EL HAJJAR, *Student member IEEE*, Guillaume GINOLHAC *Senior member IEEE*, Yajing YAN, *Member IEEE* and Mohammed Nabil EL KORSO

***Abstract*—Multi-Temporal Interferometric Synthetic Aperture Radar (MT-InSAR) exploits Synthetic Aperture Radar images time series (SAR-TS) for surface deformation monitoring via phase difference (with respect to a reference image) estimation. Most of the actual state-of-the-art MT-InSAR rely on temporal covariance matrix of the SAR-TS, assuming Gaussian distribution. However, these approaches become computationally expensive when the time series lengthens and new images are added to the data vector. This paper proposes a novel approach to sequentially integrate each newly acquired image using Phase Linking (PL) and Maximum Likelihood Estimation (MLE). The methodology divides the data into blocks, using previous images and estimations as a prior to sequentially estimate the phase of the new image. Actually, this framework allows to consider non Gaussian distributions, such as a mixture of scaled Gaussian distribution, which is particularly important to consider when dealing with urban areas.**

***Index Terms*—Multi-Temporal Interferometric Synthetic Aperture Radar, Maximum Likelihood Estimation, covariance matrix estimation, mixture of Scaled Gaussian distribution**

I. Introduction

Interferometric Synthetic Aperture Radar (InSAR) analysis, a pivotal technique in Synthetic Aperture Radar (SAR) imagery, is widely employed for various applications such as monitoring volcanoes and earthquakes, assisting in construction and urban planning, investigating the effects of climate changes, among others. This technique operates by transmitting radar waves from the satellite to the ground and capturing the backreflected echoes. Ground movements with high accuracy can be detected by comparing phases of SAR images acquired at two different dates (2-pass InSAR). However, this technique shows limitations when image acquisitions become distant, which results in coherence loss, thus information loss. Multi-Temporal Interferometric Synthetic Aperture Radar (MT-InSAR) approaches offer enhanced performances compared to the 2-pass approach. One of the most widely used approaches in MT-InSAR is Phase Linking (PL), which exploits the full covariance matrix of Synthetic Aperture Radar images time series (SAR-TS) and their statistical properties. The first objective of PL approaches consists of estimating the phase differences relative to a reference image from the SAR-TS, with improved accuracy and respecting the temporal phase closure. For this, early PL approaches require prior knowledge on coherence matrix and take the modulus of the Sample Covariance Matrix (SCM) as a plug-in for the coherence matrix [1]. This approach is equivalent to taking the Maximum Likelihood Estimation (MLE) of the covariance matrix without considering its structure (see equation (2)) which makes it a suboptimal estimator due to the use of the modulus operator which is non-holomorphic. To correct this issue, a true MLE framework has been proposed in [2], where the coherence and the phases are estimated by a 1-step approach. The proposed solution involves using iterative algorithms such as Block Coordinate Descent (BCD) including a Majorization-Minimization (MM). An extension to non Gaussian data has been proposed [3], which shows their interest in urban areas where the Gaussian assumption is often no longer valid [4]. However, this algorithm remains computationally intensive, particularly due to use of iterative procedures and complex mathematical operations on matrices that grow in size over time. Additionally, it is unable to efficiently handle the integration of new images and requires a complete re-estimation of all phases of the time series as well as the covariance matrix, which in this case corresponds to the Tyler estimator, which itself is computationally expensive to calculate. This becomes a real issue especially with the vast amount of available SAR images thanks to ongoing SAR missions.

Recently, online signal processing algorithms have seen a great attraction and interest due to their ability to process data continuously in real time, unlike batch algorithms that require additional time to gather sufficient samples [5–8]. This real-time ability eliminates the need for complex and resource-intensive operations, making online approaches a more efficient and cost-effective solution.

To the best of our knowledge, sequential processing of SAR-TS has not been extensively explored. One straightforward approach is to consider phase differences only between the new image and several previous images with close acquisition dates, like the Small BAseline Subset (SBAS) method [9] which pairs SAR images with small temporal baselines. However, this approach can introduce phase bias due to the presence of short-lived fading signals [10]. One notable sequential approach was proposed in [11], where the idea is to divide the SAR-TS into mini-stacks and apply the classic PL to each mini-stack. The mini-stacks are then compressed into a single virtual image through Principal Component Analysis (PCA). Each mini-stack is treated relative to its first image, a global PL is performed to link all the mini-stacks through the compressed version of each mini-stack. This approach use PL within a Gaussian framework and necessites the determination of an appropriate period for sufficient SAR image acquisition.

In this paper, we propose a sequential approach based on [3], which leverages the benefits of the MLE over classic PL while maintaining a lower computational cost. It generalizes the approach proposed in [12], namely Sequential Phase Linking based on Maximum Likelihood Estimation for a Gaussian

"This work is funded by the ANR REPED-SARIX project (ANR-21-CE23-0012-01) of the French national Agency of research." The source code is available on GitHub at the following address: https://github.com/DanaElhajjar/S-SG-MLE-PL

model (S-G-MLE-PL), to a Non-Gaussian model.

In this paper, we present a robust sequential approach. Specifically, the previous images along with their corresponding estimated parameters are used as prior information, allowing us to leverage the conditional distribution of the new image relative to the previous ones. Our approach resembles those used in handling missing data, where prior information plays a crucial role [13, 14]. Closed-form solutions for each parameter are derived and computed using a BCD algorithm. Our approach demonstrates similar performance to traditional offline methods in both simulations and real data studies, while also significantly reducing computational costs.

In the continuation of the paper, the exponent ^{T} (resp. *) denotes the transposed operator (resp. the conjugated operator), while the symbol $\circ$ characterizes the element-wise (Hadamard) multiplication, and the exponent ^{H} corresponds to the transposed and complex conjugated operator (Hermitian). Matrices are written in bold uppercase, vectors in bold lowercase, and scalars in lowercase.

II. SAR IMAGE TIME SERIES MODEL

For a given stack of $l = p + 1$ SAR images, we consider a local homogeneous spatial neighborhood of size n denoted $\{\widetilde{\mathbf{x}}^i\}_{i=1}^n$ where $\widetilde{\mathbf{x}}^i \in \mathbb{C}^l$ for all $i \in [\![1, n]\!]$, i.e.,

$$\widetilde{\mathbf{x}}^i = [\underbrace{x_1^i, \ldots, x_p^i}_{\mathbf{x}^i}, x_l^i]^T \in \mathbb{C}^l, \tag{1}$$

$\mathbf{x}^i \in \mathbb{C}^p$ indicates the multivariate pixel of the previous images (Fig. 1). A common assumption consists in considering

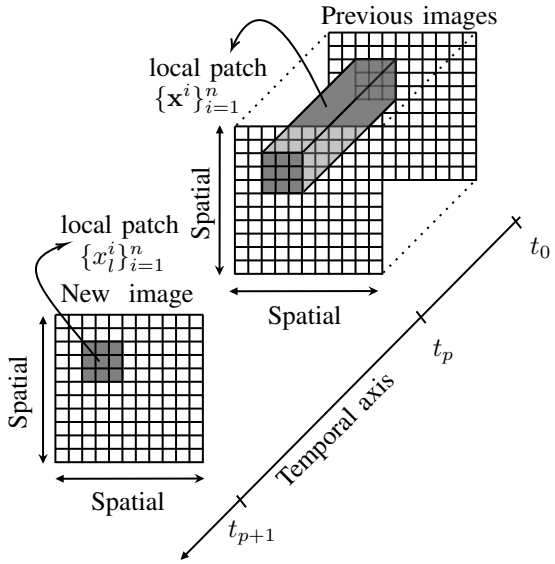

Fig. 1: The representation of SAR data incorporates both previous and recently acquired images. The local neighborhood of size n is denoted by gray pixels (sliding window).

that $\{\widetilde{\mathbf{x}}^i\}_{i=1}^n$ is a set of vectors independent and identically distributed (i.i.d) following a zero mean Complex Circular Gaussian (CCG) distribution [15], i.e., $\widetilde{\mathbf{x}} \sim \mathcal{CN}(0, \widetilde{\mathbf{\Sigma}})$. Most of PL algorithms in the literature are based on this assumption [2, 16–18], however [3, 4] showed that this assumption does not always hold true and addressed Scaled Gaussian model. For this scenario, the data follows a Gaussian distribution conditionally to a deterministic unknown scale τ_i [19, 20], i.e, $\widetilde{\mathbf{x}}^i \sim \mathcal{CN}(0, \tau_i\widetilde{\mathbf{\Sigma}})$. The real core of the covariance matrix is denoted by $\widetilde{\mathbf{\Psi}}$, and $\widetilde{\mathbf{w}}_\theta$ represents the vector of the exponential of the complex phases ($\widetilde{\mathbf{w}}_\theta = [e^{j\theta_0}, \ldots, e^{j\theta_l}]$). Based on standard physical parameters in InSAR, the covariance matrix respects the given structure [1]

$$\widetilde{\mathbf{\Sigma}} = \widetilde{\mathbf{\Psi}} \circ \widetilde{\mathbf{w}}_\theta \widetilde{\mathbf{w}}_\theta^H. \tag{2}$$

According to (2) and given the representation of the data in (1), the covariance matrix can be equivalently represented as

$$\widetilde{\mathbf{\Sigma}} = \begin{pmatrix} \mathbf{\Sigma} & w_{\theta_l}^* \mathrm{diag}(\mathbf{w}_\theta)\boldsymbol{\gamma}^T \\ \boldsymbol{\gamma}\mathrm{diag}(\mathbf{w}_\theta)^H w_{\theta_l} & \gamma_l \end{pmatrix}, \tag{3}$$

where $\mathbf{\Sigma}$ corresponds to the previously estimated covariance matrix between the previous SAR images, $\boldsymbol{\gamma}$ denotes the coherence vector between the newly acquired data and the previous ones, γ_l symbolizes the variance of the newly acquired data, and w_{θ_l} is the exponential of the phase of the latest date and $\mathbf{w}_\theta$ corresponds to the vector of the exponential of the complex phases differences of the past.

III. OFFLINE APPROACHES

PL approach consists in estimating the SAR wrapped phases while exploiting the covariance matrix of the SAR image time series, making it an inferential statistical procedure. Starting from l SAR images, PL algorithms aim to estimate $l-1$ phases differences from all possible combinations ($\frac{l(l-1)}{2}$), which is equivalent to combining all interferometric phases into a single reference. This algorithm underwent updates and enhancements over the years [1, 3, 17, 18, 21, 22]. A recent review of PL algorithms was proposed in [23, 24]. The classic PL [1] algorithms start by calculating the SCM, $\widetilde{\mathbf{S}} = \frac{1}{n}\sum_{i=1}^n \widetilde{\mathbf{x}}^i \widetilde{\mathbf{x}}^{iH}$, and then considering $\widetilde{\mathbf{\Psi}} = |\widetilde{\mathbf{S}}|$ as a plug-in of the coherence matrix in order to solve the following problem

$$\begin{aligned} \underset{\widetilde{\mathbf{w}}_\theta}{\text{minimize}} \quad & \mathcal{L}(\widetilde{\mathbf{\Psi}} \circ \widetilde{\mathbf{w}}_\theta \widetilde{\mathbf{w}}_\theta^H) \\ \text{subject to} \quad & \widetilde{\mathbf{w}}_\theta \in \mathbb{T}_l, \widetilde{w}_{\theta_1} = 1 \end{aligned} \tag{4}$$

where $\mathcal{L}$ corresponds to the negative log-likelihood function of the data following the zero mean CCG distribution. $\mathbb{T}_l = \left\{\widetilde{\mathbf{w}}_\theta \in \mathbb{C}^l \,|\, |[\widetilde{\mathbf{w}}_\theta]_i| = 1, \forall i \in [1, l]\right\}$ is the l-torus of phase only complex vectors. The classic PL relies on the coherence matrix plug-in which can biases the results especially in case of low coherence regions, heterogeneous samples or small sample size. To address these issues, [2, 3, 18] proposed to use the MLE of the coherence matrix along with the phases which allows solving the following problem by the BCD [25]. The latter reads as

$$\begin{aligned} \underset{\widetilde{\mathbf{\Psi}}, \widetilde{\mathbf{w}}_\theta}{\text{minimize}} \quad & \mathcal{L}(\widetilde{\mathbf{\Psi}} \circ \widetilde{\mathbf{w}}_\theta \widetilde{\mathbf{w}}_\theta^H) \\ \text{subject to} \quad & \widetilde{\mathbf{\Psi}} \in \mathbb{R}^{l\times l}, \widetilde{\mathbf{w}}_\theta \in \mathbb{T}_l, \widetilde{w}_{\theta_1} = 1 \end{aligned} \tag{5}$$

The coherence matrix $\widetilde{\mathbf{\Psi}}$ can be given in a closed-form, and $\widetilde{\mathbf{w}}_\theta$ can be found through a MM algorithm [26, 27]. This algorithm exhibits favorable convergence properties [28], which can be attributed to the same arguments as in [29, 30], given its constraint within the compact set $\mathbb{T}_l$. This approach can be extended to a mixture of Scaled Gaussian models [19] where

$\widetilde{\mathbf{x}}^i \sim \mathcal{CN}(0, \tau_i \widetilde{\mathbf{\Sigma}})$. This offline algorithm will be denoted in the following MLE-PL [3].

IV. Proposed sequential approach

In our approach, namely S-MLE-PL hereafter, the coherence parameters, γ_l and $\boldsymbol{\gamma}$, are estimated simultaneously with the phase of the new image w_{θ_l} and the deterministic scale τ_i, as

$$\begin{aligned} \min_{\boldsymbol{\gamma},\gamma_l,w_{\theta_l},\{\tau_i\}_{i=1}^n} \quad & \mathcal{L}(\{\widetilde{\mathbf{x}}^i\}_{i=1}^n;\boldsymbol{\gamma},\gamma_l,w_{\theta_l},\{\tau_i\}_{i=1}^n) \\ \text{subject to} \quad & \boldsymbol{\gamma}\in\mathbb{R}^p, \gamma_l\in\mathbb{R}, |w_{\theta_l}|=1,\ \theta_1=0 \end{aligned} \tag{6}$$

The objective function of the aforementioned problem is the negative log-likelihood for the entire data set. Given the covariance matrix structure in (3) and assuming that $\widetilde{\mathbf{x}}^i \sim \mathcal{CN}(0, \tau_i \widetilde{\mathbf{\Sigma}})$, the negative log-likelihood derived from these assumptions for the entire data set, can be expressed as

$$\begin{aligned} \mathcal{L}(\{\widetilde{\mathbf{x}}^i\}_{i=1}^n;\boldsymbol{\gamma},\gamma_l,w_{\theta_l},\{\tau_i\}_{i=1}^n) &= -\sum_{i=1}^n \mathcal{L}(\widetilde{\mathbf{x}}^i;\boldsymbol{\gamma},\gamma_l,w_{\theta_l},\tau_i) \\ &= -\sum_{i=1}^n \left[\mathcal{L}(x_l^i|\mathbf{x}^i;\boldsymbol{\gamma},\gamma_l,w_{\theta_l},\tau_i) + \mathcal{L}(\mathbf{x}^i;\tau_i)\right] \end{aligned} \tag{7}$$

In the above equation, the transition from the distribution over the entire dataset to the conditional distribution is achieved through [31], where $x_l^i|\mathbf{x}^i \sim \mathcal{CN}(\mu_x^i, \sigma_x^2)$ in which

- $\mu_x^i = w_{\theta_l}\boldsymbol{\gamma}\text{diag}(\hat{\mathbf{w}}_\theta)^H\hat{\mathbf{\Sigma}}^{-1}\mathbf{x}^i$
- $\sigma_x^2 = \tau_i(\gamma_l - \boldsymbol{\gamma}\text{diag}(\hat{\mathbf{w}}_\theta)^H\hat{\mathbf{\Sigma}}^{-1}\text{diag}(\hat{\mathbf{w}}_\theta)\boldsymbol{\gamma}^T)$

where $\hat{\mathbf{w}}_\theta$ and $\hat{\mathbf{\Sigma}}$ were previously estimated using the offline MLE-PL method [3] based on previous images $\{\mathbf{x}^i\}_{i=1}^n$.By denoting $k = \boldsymbol{\gamma}\text{diag}(\hat{\mathbf{w}}_\theta)^H\hat{\mathbf{\Sigma}}^{-1}\text{diag}(\hat{\mathbf{w}}_\theta)\boldsymbol{\gamma}^T$, $v = \gamma_l - k$, $\mathbf{L}^i = \mathbf{x}^{iH}\hat{\mathbf{\Sigma}}^{-1}\text{diag}(\hat{\mathbf{w}}_\theta)$, $y^i = x_l^i - w_{\theta_l}\boldsymbol{\gamma}\mathbf{L}^{iH}$

$$\begin{aligned} \mathcal{L}(\{\widetilde{\mathbf{x}}^i\}_{i=1}^n;\boldsymbol{\gamma},\gamma_l,w_{\theta_l},\{\tau_i\}_{i=1}^n) = \sum_{i=1}^n \Bigg[& l\log(\tau_i) + \log(v) \\ & + \frac{y^{i*}y^i}{\tau_i v} + \frac{1}{\tau_i}\mathbf{x}^{iH}\hat{\mathbf{\Sigma}}^{-1}\mathbf{x}^i\Bigg] \end{aligned} \tag{8}$$

The problem (6) can be solved using a BCD algorithm [25]. It updates iteratively each parameter by solving the corresponding sub-problem while holding the other parameters fixed (cf. Algorithm 1). The convergence of the BCD algorithm is guaranteed in this case since each sub-problem is convex [25, 28].

Algorithm 1 BCD algorithm

input : Samples $\{\widetilde{\mathbf{x}}^i\}_{i=1}^n$, $\hat{\mathbf{\Sigma}}$, $\text{diag}(\hat{\mathbf{w}}_\theta)$
initialization :$\{\tau_i\}_{i=1}^n = 1$, $w_{\theta_l} = 1$, $\boldsymbol{\gamma}$ and γ_l using the Toeplitz matrix structure
repeat
  Bloc 1 : Update of $\{\tau_i\}_{i=1}^n$ with (10)
  Bloc 2 : Update of $\boldsymbol{\gamma}$ with (12)
  Bloc 3 : Update of γ_l with (14)
  Bloc 4 : Update of w_{θ_l} with (16)
until convergence
output: $\boldsymbol{\gamma}$, γ_l and w_{θ_l}

In the following, we present the results of the updates. The detailed calculation procedures throughout the article are provided in the supplementary materials.

Bloc 1 : Update $\{\tau_i\}_{i=1}^n$

By fixing $\boldsymbol{\gamma}$, γ_l and w_{θ_l}, the problem of updating $\{\tau_i\}_{i=1}^n$ can be formulated as follows

$$\min_{\{\tau_i\}_{i=1}^n} \quad \sum_{i=1}^n \left[l\log(\tau_i) + \frac{y^{i*}y^i}{\tau_i v} + \frac{1}{\tau_i}\mathbf{x}^{iH}\hat{\mathbf{\Sigma}}^{-1}\mathbf{x}^i\right] \tag{9}$$

The corresponding analytical solution is

$$\tau_i = \frac{y^{i*}y^i}{lv} + \frac{\mathbf{x}^{iH}\hat{\mathbf{\Sigma}}^{-1}\mathbf{x}^i}{l}, \tag{10}$$

Bloc 2 : Update $\boldsymbol{\gamma}$

$\boldsymbol{\gamma}$ is updated by fixing γ_l, w_{θ_l} and $\{\tau_i\}_{i=1}^n$, with the following sub-problem

$$\min_{\boldsymbol{\gamma}} \quad \sum_{i=1}^n \left[\log(v) + \frac{y^{i*}y^i}{\tau_i v}\right] \quad \text{s.t.} \quad \boldsymbol{\gamma}\in\mathbb{R}^p \tag{11}$$

and by designating $\mathbf{M}^i = \mathbf{L}^{iH}\mathbf{L}^i$, the analytical resolution takes the following form

$$\boldsymbol{\gamma} = \left(\sum_{i=1}^n \tfrac{1}{\tau_i}(w_{\theta_l}^* x_l^i\mathbf{L}^i - w_{\theta_l}x_l^{i*}\mathbf{L}^{i*})\right).\left(\sum_{i=1}^n \tfrac{1}{\tau_i}(\mathbf{M}^{i*} + \mathbf{M}^i)\right)^{-1}, \tag{12}$$

Bloc 3 : Update γ_l

The problem of updating γ_l with fixed $\{\tau_i\}_{i=1}^n$, $\boldsymbol{\gamma}$ and w_{θ_l} reads

$$\min_{\gamma_l} \quad \sum_{i=1}^n \left[\log(v) + \frac{y^{i*}y^i}{\tau_i v}\right] \quad \text{s.t.} \quad \gamma_l\in\mathbb{R} \tag{13}$$

The minimizer is obtained as

$$\gamma_l = \frac{1}{n}\sum_{i=1}^n \frac{1}{\tau_i}(x_l^i - w_{\theta_l}\boldsymbol{\gamma}\mathbf{L}^{iH})^*(x_l^i - w_{\theta_l}\boldsymbol{\gamma}\mathbf{L}^{iH}) + k, \tag{14}$$

Bloc 4 : Update w_{θ_l}

Updating w_{θ_l} with fixed $\{\tau_i\}_{i=1}^n$, $\boldsymbol{\gamma}$ and γ_l requires to solve the sub-problem

$$\min_{w_{\theta_l}} \quad \sum_{i=1}^n \frac{y^{i*}y^i}{\tau_i v} \quad \text{s.t.} \quad |w_{\theta_l}| = 1 \tag{15}$$

The phase difference of the new image has the following form

$$w_{\theta_l} = \left((\sum_{i=1}^n \frac{1}{\tau_i^*}x_i\mathbf{L}^i\boldsymbol{\gamma}^T).(\sum_{i=1}^n \frac{1}{\tau_i^*}\boldsymbol{\gamma}\mathbf{M}^i\boldsymbol{\gamma}^T)^{-1}\right). \tag{16}$$

A projection step is required to respect the constraint in the sub-problem (15).

Computational cost: PL approach is expensive, mainly due to the number of images involved, the latter increases the size of the coherence matrix and extends computations time due to extensive mathematical matrix operations. Offline approaches handle inversion and estimating $l \times l$ matrices, while our approach focuses on estimating scalars and one vector. The complexity of the S-MLE-PL approach is $O(p^3)$, while the complexity of the MLE-PL approach is $O(n_{\text{iter}}l^3)$.

V. Method Evaluation

A. Synthetic data

A time series of $l = p + 1 = 20$ images is simulated. The covariance matrix is generated according to (2), where $\tilde{\mathbf{\Psi}}$ is simulated as a Toeplitz matrix i.e., $[\tilde{\mathbf{\Psi}}]_{ij} = \rho^{|i-j|}$ with a coefficient correlation $\rho = 0.7$. In the matrix $\tilde{\mathbf{\Psi}}$, the coherence between the new image and the previous ones, $\boldsymbol{\gamma}$, corresponds

to the last row and the scalar at (l, l) position corresponds to the variance of the new image γ_l. We simulate linearly l SAR phases between 0 and 2π, i.e., $\Delta_{i,i-1} = \theta_i - \theta_{i-1} = 2/l$ rad. The n i.i.d samples are then simulated as $\tilde{\mathbf{x}}^i \sim \mathcal{CN}(0, \tau_i \tilde{\mathbf{\Sigma}})$, where each τ_i is sampled according to a Gamma distribution $\tau \sim \Gamma(\nu, \frac{1}{\nu})$ with $\nu = 0.1$. The scale parameter $v \in \mathbb{R}^+$ governs the tail of the distribution. When the value of ν is small (e.g., $\nu = 0.1$), the simulated data become highly heterogeneous, which is desirable as it aligns with the characteristics of urban areas in the real world. However, if the data are Gaussian ($v \to \infty$), similar to natural environments, the method produces results identical to those of a Gaussian model based approach, since in covariance matrix estimation, non-Gaussian estimators perform similarly to Gaussian estimators under a Gaussian distribution [32, 33].We compare our results with those obtained from other state-of-the-art approaches: classic PL [24] and MLE-PL [3]. We consider the Mean Squared Error (MSE) which is computed using 1000 Monte Carlo trials.

1) Comparison with offline approaches

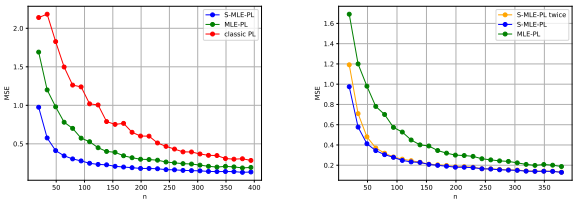

(a) Comparison with offline approaches (b) Sequential integration of several new images

Fig. 2: MSE of phase difference estimation between the 1^{st} and 20^{th} (last) dates for $l = 20$ with respect to increasing sample size (n) using 1000 Monte Carlo trials.

Fig. 2a represents the MSE of phase estimates for a sample size $n = 64$ when n increases. As foreseen, the larger the sample size, the better the performances are in terms of MSE for all approaches. Offline approaches require operations on large matrices, such as matrix inversion which is sensitive to the samples size. The sequential approach shows better results particularly on small sample size. For low sample support ($n < 100$), S-MLE-PL shows better performance than classic PL and MLE-PL. In this paper, we compare the sequential and offline approaches, highlighting the potential for parameter ν variation.

2) Sequential integration of several new images

We compare 3 setups: (a) offline processing (MLE-PL): processing the entire set together, (b) partial sequential processing (S-MLE-PL): the last phase is estimated with the proposed approach and (c) full sequential processing (S-MLE-PL twice): the last 2 images are added sequentially and the S-MLE-PL is used twice. We show that the full sequential processing outperforms the offline processing (MLE-PL), and performs comparably to adding one observation at a time (Fig. 2b).

B. Real data

Mexico city is considered one of the densely populated urban areas with a population that surpasses 20 million. Consequently, Mexico city faces significant challenges related to water management frequently encountering situations where water demand exceeds the available supply. To address this issue, the city relies on groundwater extraction leading to occurrences of subsidence and deformations in the land. We investigate a pile of 20 Sentinel-1 SAR images covering Mexico city, acquired every 12 days from August 14, 2019, to April 10, 2020 to evaluate the effectiveness of the proposed approach. Fig. 3 presents the longest temporal baseline interferogram estimated by MLE-PL [3], S-MLE-PL, with the multi-looking window, denoted as $n = 8 \times 8$, remains the same. The results are analyzed by comparing MLE-PL with our sequential approach. Both approaches, MLE-PL and S-MLE-PL yield the same results, however the sequential approach demonstrates significantly faster execution time compared to the offline one when applied to real data. Practically, the sequential approach took only 0.094 hour, whereas the offline method required over 0.78 hour using a machine with a 95-core CPU running at 2.2 GHz and 125 G of RAM with calculations executed in parallel across the CPUs. Additionally, we compare the results of our approach with those of [12] and [11]. Based on [11], which used the Root Mean Squared Error (RMSE) criterion despite the ambiguity of the modulo 2π in phase estimation, we compute the RMSE between these sequential approaches and the offline result MLE-PL [3]. We observe that our approach yields a lower value of $\text{RMSE}_{\text{S-MLE-PL}} = 1.62$, while $\text{RMSE}_{\text{S-G-MLE-PL}} = 1.74$ and the Sequential Estimator [11] has an $\text{RMSE}_{\text{Seq Est}} = 1.89$.

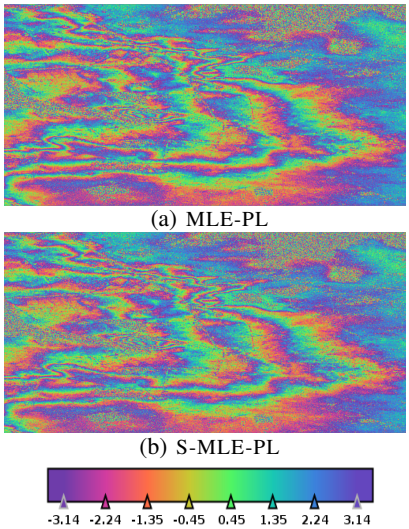

(a) MLE-PL

(b) S-MLE-PL

Fig. 3: Close-up view of the longest temporal baseline interferogram (14 August 2019 - 10 April 2020) estimated by (a) MLE-PL [3] and (b) S-MLE-PL in case $l = 20$ and $n = 64$.

VI. Conclusion

In this paper, a novel sequential PL approach is proposed to estimate the phase difference in InSAR based on a MLE framework. The estimator stands out for its robustness within the considered Scaled Gaussian model and improved performance is observed in both simulations and real-world data, demonstrating enhanced estimation efficiency in terms of accuracy and computational cost.

REFERENCES

[1] A. Guarnieri and S. Tebaldini, "On the exploitation of target statistics for SAR interferometry applications," *IEEE Transactions on Geoscience and Remote Sensing*, vol. 46, no. 11, pp. 3436–3443, 2008.

[2] P. Vu, F. Brigui, A. Breloy, Y. Yan, and G. Ginolhac, "A new phase linking algorithm for multi-temporal InSAR based on the maximum likelihood estimator," in *IGARSS*. IEEE, 2022, pp. 76–79.

[3] P. Vu, A. Breloy, F. Brigui, Y. Yan, and G. Ginolhac, "Robust phase linking in InSAR," *IEEE Transactions on Geoscience and Remote Sensing*, vol. 61, pp. 1–11, 2023.

[4] A. Mian, G. Ginolhac, J-P. Ovarlez, and A.M. Atto, "New robust statistics for change detection in time series of multivariate SAR images," *IEEE Transactions on Signal Processing*, vol. 67, no. 2, pp. 520–534, 2018.

[5] Y.V. Zakharov, G.P. White, and J. Liu, "Low-complexity rls algorithms using dichotomous coordinate descent iterations," *IEEE Transactions on Signal Processing*, vol. 56, no. 7, pp. 3150–3161, 2008.

[6] D. Angelosante, J.A. Bazerque, and G.B. Giannakis, "Online adaptive estimation of sparse signals: Where RLS meets the ℓ_1-norm," *IEEE Transactions on Signal Processing*, vol. 58, no. 7, pp. 3436–3447, 2010.

[7] F. Elvander, J. Swärd, and A. Jakobsson, "Online estimation of multiple harmonic signals," *IEEE ACM Transactions on Audio, Speech, and Language Processing*, vol. 25, no. 2, pp. 273–284, 2016.

[8] Y. Zhang, Y. Huang, Y. Zhang, S. Liu, J. Luo, X. Zhou, J. Yang, and A. Jakobsson, "High-throughput hyperparameter-free sparse source location for massive tdm-mimo radar: Algorithm and FPGA implementation," *IEEE Transactions on Geoscience and Remote Sensing*, 2023.

[9] R. Lanari, O. Mora, M. Manunta, J.J. Mallorquí, P. Berardino, and E. Sansosti, "A small-baseline approach for investigating deformations on full-resolution differential SAR interferograms," *IEEE Transactions on Geoscience and Remote Sensing*, vol. 42, no. 7, pp. 1377–1386, 2004.

[10] H. Ansari, F. De Zan, and A. Parizzi, "Study of systematic bias in measuring surface deformation with SAR interferometry," *IEEE Transactions on Geoscience and Remote Sensing*, vol. 59, no. 2, pp. 1285–1301, 2020.

[11] H. Ansari, F. De Zan, and R. Bamler, "Sequential estimator: Toward efficient InSAR time series analysis," *IEEE Transactions on Geoscience and Remote Sensing*, vol. 55, no. 10, pp. 5637–5652, 2017.

[12] D. El Hajjar, Y. Yan, G. Ginolhac, and M.N. El Korso, "Sequential phase linking: progressive integration of SAR images for operational phase estimation," in *IGARSS*. IEEE, 2024.

[13] A. Aubry, A. De Maio, S. Marano, and M. Rosamilia, "Structured covariance matrix estimation with missing-(complex) data for radar applications via expectation-maximization," *IEEE Transactions on Signal Processing*, vol. 69, pp. 5920–5934, 2021.

[14] A. Hippert-Ferrer, M.N. El Korso, A. Breloy, and G. Ginolhac, "Robust low-rank covariance matrix estimation with a general pattern of missing values," *Signal Processing*, vol. 195, pp. 108460, 2022.

[15] R. Bamler and P. Hartl, "Synthetic aperture radar interferometry," *Inverse problems*, vol. 14, no. 4, pp. R1, 1998.

[16] A. Ferretti, C. Prati, and F. Rocca, "Permanent scatterers in SAR interferometry," *IEEE Transactions on Geoscience and Remote Sensing*, vol. 39, no. 1, pp. 8–20, 2001.

[17] H. Ansari, F. De Zan, and R. Bamler, "Efficient phase estimation for interferogram stacks," *IEEE Transactions on Geoscience and Remote Sensing*, vol. 56, no. 7, pp. 4109–4125, 2018.

[18] C. Wang, X. Wang, Y. Xu, Bochen Zhang, M. Jiang, S. Xiong, Q. Zhang, W. Li, and Q. Li, "A new likelihood function for consistent phase series estimation in distributed scatterer interferometry," *IEEE Transactions on Geoscience and Remote Sensing*, vol. 60, pp. 1–14, 2022.

[19] E. Ollila, D.E. Tyler, V. Koivunen, and H.V. Poor, "Complex elliptically symmetric distributions: Survey, new results and applications," *IEEE Transactions on Signal Processing*, vol. 60, no. 11, pp. 5597–5625, 2012.

[20] V.J. Yohai R.A. Maronna, R.D. Martin and M. Salibián-Barrera, *Robust statistics: theory and methods (with R)*, John Wiley & Sons, 2019.

[21] Z. Gao, X. He, Z. Ma, S. Wei, J. Xiong, and Y. Aoki, "Distributed scatterer interferometry for fast decorrelation scenarios based on sparsity regularization," *IEEE Transactions on Geoscience and Remote Sensing*, 2024.

[22] A. Ferretti, A. Fumagalli, F. Novali, C. Prati, F. Rocca, and A. Rucci, "A new algorithm for processing interferometric data-stacks: SqueeSAR," *IEEE Transactions on Geoscience and Remote Sensing*, vol. 49, no. 9, pp. 3460–3470, 2011.

[23] D. Minh and S. Tebaldini, "Interferometric phase linking: Algorithm, application, and perspective," *IEEE GRSM*, vol. 11, no. 3, pp. 46–62, 2023.

[24] N. Cao, H. Lee, and H. Jung, "Mathematical framework for phase-triangulation algorithms in distributed-scatterer interferometry," *IEEE GRSL*, vol. 12, no. 9, pp. 1838–1842, 2015.

[25] M. Hong, M. Razaviyayn, Z.Q. Luo, and J.S. Pang, "A unified algorithmic framework for block-structured optimization involving big data: With applications in machine learning and signal processing," *IEEE Signal Processing Magazine*, vol. 33, no. 1, pp. 57–77, 2015.

[26] D.R. Hunter and K. Lange, "A tutorial on MM algorithms," *The American Statistician*, vol. 58, no. 1, pp. 30–37, 2004.

[27] P. Babu Y. Sun and D.P. Palomar, "Majorization-minimization algorithms in signal processing, communications, and machine learning," *IEEE Transactions on Signal Processing*, vol. 65, no. 3, pp. 794–816, 2016.

[28] M. Razaviyayn, M. Hong, and Z.Q. Luo, "A unified convergence analysis of block successive minimization methods for nonsmooth optimization," *SIAM Journal on Optimization*, vol. 23, no. 2, pp. 1126–1153, 2013.

[29] M. Soltanalian and P. Stoica, "Designing unimodular codes via quadratic optimization," *IEEE Transactions on Signal Processing*, vol. 62, no. 5, pp. 1221–1234, 2014.

[30] A. Breloy, S. Kumar, Y. Sun, and D.P. Palomar, "Majorization-minimization on the Stiefel manifold with application to robust sparse PCA," *IEEE Transactions on Signal Processing*, vol. 69, pp. 1507–1520, 2021.

[31] T. W. Anderson, "An introduction to multivariate statistical analysis," Tech. Rep., 1965.

[32] F. Pascal, J.P. Barbot, H. Harari-Kermadec, R. Suyama, and P. Larzabal, "An empirical likelihood method for data aided channel identification in unknown noise field," in *2008 16th European Signal Processing Conference*. IEEE, 2008, pp. 1–5.

[33] H. Harari-Kermadec and F. Pascal, "On the use of empirical likelihood for non-gaussian clutter covariance matrix estimation," in *2008 IEEE Radar Conference*. IEEE, 2008, pp. 1–6.